ORIGINAL ARTICLE

Systematic Development of Hot Melt Extrusion-Based Amorphous Solid Dispersion: Integrating Quality by Design and In Silico Modeling

Anuj Kumar Fanda[1,2] · Ajinkya Jadhav[1] · Pushpendra S. Naruka[2] · Dhwani Rana[3] · Derajram Benival[3]

Abstract

Purpose The study aimed to develop and optimize apremilast (APST) solid dispersion formulations using copovidone (Kollidon VA64) as the carrier and vitamin E TPGS as the surfactant to enhance solubility and dissolution, and to utilize in silico Physiologically Based Biopharmaceutics Modeling (PBBM) in GastroPlus to simulate the in vivo behaviour of the optimized formulation, predicting its potential for enhancing oral bioavailability.

Methods Solid dispersion formulations of APST were prepared via the hot melt extrusion (HME) technique, utilizing copovidone (commercially known as Kollidon VA64) as the polymeric carrier. The selection of suitable polymeric carriers as well as surfactant was initially performed through phase solubility studies. The second-generation amorphous solid dispersion (ASD) was formulated with Kollidon VA64. Following this, the third-generation solid dispersions were engineered by choosing vitamin E TPGS as the surfactant carrier, a decision informed by comprehensive screening studies. The formulation of these batches employed a twin-screw configuration in the HME process. Design of Experiments (DoE) approach was utilized to ascertain the optimal ratio of drug: polymer: surfactant to achieve maximum solubility and dissolution enhancement. Drug release studies were conducted in 6.8 phosphate buffer solution. The developed formulations were subjected to a variety of characterization techniques to assess their properties. Stability studies were conducted for the final formulation over a period of up to three months.

Results Based on the DoE studies, the optimized formulation was identified as APST with copovidone (Kollidon VA64) in a 1:5 ratio, supplemented with 3% vitamin E TPGS. Furthermore, PBBM in GastroPlus was utilized to simulate the in vivo behaviour of the optimized formulation.

Conclusion The amorphous solid dispersion (ASD) of APST, developed via the HME technique, demonstrated a substantial enhancement in solubility, exhibiting an increase of up to 248-fold relative to the unprocessed drug over a 24-hour period. A noteworthy increase in the percentage of drug release during dissolution was observed in comparison to the pure drug. The observed improvements in solubility and dissolution were corroborated through PBBM in GastroPlus, thereby suggesting a viable strategy for enhancing the oral bioavailability of APST. This investigation effectively illustrates the formulation of a third-generation ASD of APST, significantly ameliorating its solubility and pharmacokinetic parameters, and indicating potential for industrial-scale manufacturing.

Keywords Hot melt extrusion · Amorphous solid dispersion · In silico · Modelling · DoE

✉ Anuj Kumar Fanda
anujfanda@yahoo.co.in

✉ Derajram Benival
derajram@niperahm.res.in

1 Sun Pharmaceutical Industries Limited, R&D, Sarhaul, Sec 18, Gurgaon, Haryana 122015, India

2 Bhupal Noble's University, Udaipur, Rajasthan, India

3 Department of Pharmaceuticals, National Institute of Pharmaceutical Education and Research (NIPER-A), An Institute of National Importance, Government of India, Ministry of Chemicals and Fertilizers, Opp. Airforce Station, Palaj, Gandhinagar, Ahmedabad, Gujarat 382355, India

Introduction

The field of pharmaceutical science has been persistently challenged by the issue of poor solubility associated with a significant proportion (> 90% of R&D pipeline) of active pharmaceutical ingredients (APIs) with low solubility [1]. The advent of high throughput screening and combinatorial chemistry has led to the discovery of numerous APIs, a majority (∼50%) of which unfortunately exhibit poor solubility [2]. This poses a substantial hurdle in drug development, as poor solubility often translates to poor bioavailability, thereby limiting the therapeutic potential of these APIs. In an attempt to overcome this challenge, various strategies have been explored and employed. One such promising approach is the formulation of amorphous solid dispersions (ASDs) using the hot melt extrusion (HME) process [3]. The HME process involves the co-melting of the API and a suitable polymer, resulting in the molecular dispersion of the drug within the polymeric matrix. This amorphous dispersion significantly enhances the solubility of the API, thereby improving its bioavailability.

The mechanism of the HME process is intriguing. It utilizes the shear stress generated by screws to overcome the lattice energy of the API. This shear stress also aids in softening the polymer used in the extrusion process, facilitating the formation of a uniform amorphous dispersion. The process parameters, such as the temperature of the active ingredient and the glass transition temperature (Tg) of the polymer, play a crucial role in defining various melting zones within the extruder, thereby influencing the quality of the resulting ASD [4]. The HME process offers several advantages over other techniques, such as the solvent evaporation technique. Firstly, the HME process is a continuous process, making it more efficient and practical for both laboratory and commercial scales. Secondly, it is a solvent-free process, eliminating the need for solvent recovery and making it environmentally friendly. Thirdly, it is a dust-free process, reducing the risk of cross-contamination and improving the safety of the process. Lastly, the HME process facilitates the conversion of the final formulation into various dosage forms, including tablets, pellets, and capsules, among others, offering flexibility in dosage form design [5].

Solid dispersions can be classified into different categories based on advancements in the field. One such classification involves the distinction between generations of solid dispersions. Among the first generation of solid dispersions are those formulated with crystalline carriers. Examples of crystalline carriers commonly used include sugars and urea. These solid dispersions form crystalline structures that are thermodynamically stable and facilitate gradual drug release [6]. Second-generation solid dispersions utilize amorphous carriers instead of crystalline ones. These amorphous carriers enable the molecular distribution of the drug within the matrix. Polymeric carriers, derived from natural or synthetic sources, are predominantly employed in this generation of solid dispersions [7]. The third-generation solid dispersions employ an approach aimed at enhancing the bioavailability of drugs with low solubility. These formulations utilize a surfactant carrier or a combination of surfactants and amorphous polymers as carriers. The choice of carrier is intended to counteract drug nucleation by providing surface or emulsifying activity [7, 8].

Apremilast (APST), an oral PDE4 inhibitor, targets a variety of inflammatory mediators involved in psoriasis and psoriatic arthritis. Given the chronic nature of these diseases, long-term treatment is typically advised. APST, which is classified as a BCS class IV drug due to its poor solubility and permeability, may face limitations in its bioavailability. Additionally, the literature reports more than ten polymorphs with different physicochemical properties [9, 10]. Polymorph interconversion may further complicate the characteristics of this drug and contribute to its physicochemical instability [11]. To address these challenges, ASD technology has been employed to overcome poor solubility issues and prevent polymorphism interchange by stabilizing the drug in an amorphous state. Reports have indicated several gastrointestinal (GI) side effects, including diarrhea, nausea, and vomiting, associated with the use of APST. To mitigate these risks, dose titration is typically performed, resulting in a final dosage of twice 30 mg. Therefore, a reduced dose in response to increased solubility may help alleviate GI side effects. The primary objective of this study was to develop an ASD of APST, aiming to improve its solubility and dissolution, consequently enhancing therapeutic efficacy and oral bioavailability while potentially reducing the required dosage. This study utilized the HME approach to develop a third-generation ASD of APST.

The thermal behaviour and decomposition characteristics of APST were analyzed using Thermogravimetric Analysis (TGA), while its thermodynamic properties were investigated using Differential Scanning Calorimetry (DSC). Using Hansen solubility parameter (HSP) and Flory-Huggin (F-H) equations, the miscibility of APST with polymers was evaluated. To determine the best polymer-surfactant combinations for maximizing drug solubility, phase solubility tests were carried out. After preliminary screening experiments, Design of Experiments (DoE) approach was employed to optimize the formulation composition to achieve the maximum solubility and dissolution enhancement. Comprehensive characterization of the developed ASD was performed using techniques such as DSC, Fourier Transform Infrared Spectroscopy (FTIR), Dynamic Vapor Sorption (DVS), powder X-ray diffraction (pXRD), and scanning electron microscopy (SEM). In vitro drug release

studies were conducted to compare the release profile of the final formulation with that of the pure drug and other combinations. The final formulation was subjected to stability studies for over a period of three months to ensure that the converted ASD remains in the amorphous form at higher energy states without reverting back to its crystalline form. Pharmacokinetic parameters following oral administration were determined using Physiologically Based Biopharmaceutics Modeling (PBBM) with GastroPlus™ software. This modeling approach allowed for the simulation of oral absorption profiles for APST, offering valuable in silico insights into its pharmacokinetics.

Materials and Methods

Apremilast (APST) was gifted by Sun Pharmaceutical Industries Ltd., India, while Kollidon VA64 and Poloxamer were gifted by BASF Corporation, USA. Vitamin E TPGS was gifted by Antares Health Products, USA. Hypromellose was purchased from Dow Chemicals, USA. Acetone was purchased from SD Fine Chemicals, India. All the other reagents used in the study were of Analytical Reagent (AR) grade and were gifted by Sun Pharmaceutical Industries Ltd., India.

Thermal Gravimetric Analyis (TGA)

Thermal analysis of APST was carried out using a Thermal Gravimetric Analyzer (TA Instrument Trios Version 5.5.1.5). A sample weighing approximately 2–3 mg was measured out and evenly spread within the sample pan. The analysis involved heating a sample at a heating rate of 10 °C/min, starting at 30 °C and reaching up to 300 °C. During this process, nitrogen purging was maintained at a rate of 50 mL/min. The TGA was performed to observe the changes in sample mass with increasing temperature. The data obtained from the analysis was processed using the Universal Analysis software [12].

Determination of Thermodynamic Properties of APST

Amorphous APST was prepared in-situ in the modulated DSC (TA Instruments Q100 MDSC) through a melt quenching method. Approximately 3 mg of sample was used for analysis. This involved heating the crystalline drug from 30 °C to 170 °C with a heating rate of 10 °C/min in a hermetically sealed aluminium pan, with the temperature held isothermally at 170 °C for 5 min, followed by cooling at a rate of 120 °C/min to 0 °C. Subsequently, the sample was reheated at a rate of 10 °C/min until it reached 170 °C. This

methodology was employed to determine the Tg of APST. Notably, a similar approach was utilized by Verma et al. for the determination of the Tg of cilostazol [12].

Hansen Solubility Parameter (HSP)

The miscibility of the drug-polymer system was evaluated using the HSP [12], which involves calculating the total HSP (δ) using Eq. (1).

$$\delta^2 = \delta^2 d + \delta^2 p + \delta^2 h \tag{1}$$

where δ = total HSP, δd = dispersion HSP, δp = polar HSP and δh = hydrogen-bonded HSP

The likelihood of ASD formation via HME was predicted by applying the HSP of APST and Kollidon VA64. This prediction was based on a comparison of the solubility parameters of APST and Kollidon VA64, using values obtained from published sources [13, 14].

Calculation of Flory–Huggins (F-H) Interaction Parameter

A well-known theory that describes polymer-polymer miscibility based on the Gibbs free energy shift before and after mixing is the lattice-based F-H theory [15, 16]. F-H theory helps to calculate the miscibility of a polymer with a drug using the melting point depression method. Physical mixture of drug and polymer was prepared in a ratio of 1:1, 1:3, 1:5, 1:7 by accurately weighing the drug and polymer. The drug and polymer were sieved through an ASTM #30 (#600 μm) and thoroughly blended in a geometric manner to achieve a homogeneous mixture. The melting points of the drug-polymer combinations were analyzed using a DSC (TA Instruments - Q100 MDSC) equipped with a universal V4 5 A instrument. Prior to testing, the DSC system was purged with nitrogen at a flow rate of 70 mL/min, and calibration was performed using an Indium standard. Samples weighing approximately 3–5 mg were loaded into the DSC and subjected to a temperature range of 10 °C to 180 °C under a nitrogen blanket. The depression in the melting point of the drug in the presence of the polymer was then determined. Subsequently, the interaction parameter (χ) was calculated using Nishi–Wang's modified F-H Eq. (2) [12].

$$-\left[\frac{\Delta H}{R}\left(\frac{1}{Tm} - \frac{1}{T0m}\right) + ln\emptyset + \left(1 - \frac{1}{m}\right)(1 - \emptyset) \right] = \chi(1 - \phi)^2 \tag{2}$$

where in Tm is melting point of drug in a combination of polymers.

T$_{0m}$ is the melting point of pure drug.

R is the gas constant.

ΔH is the heat of fusion of pure drug.

Φ is volume fraction of drug.

m is volume of drug molecule where in m is calculated as Eq. (3)

$$m = \frac{Mw\,(polymer)\,/\,\rho\,(polymer)}{Mw\,(drug)\,/\,\rho\,(drug)} \qquad (3)$$

Mw and ρ are molecular weight and density of drug and polymer

χ is drug polymer interaction parameter.

Value of slope on left side of equation against $(1-\phi)^2$ provides the interaction parameter.

Phase Solubility Studies

Studies on solubility were conducted by mixing purified water with increasing amounts (0–10% w/v) of copovidone (Kollidon VA 64), hypromellose, vitamin E TPGS, and poloxamer with extra APST. The mixtures were sealed hermetically in glass vials and placed in a shaker incubator (Colton India) for 24 h at 37 °C ± 0.5 °C. A polyvinylidene fluoride (PVDF) filter with a 0.45 μm pore size was used to filter the samples. The initial few mL of sample were discarded. The concentration in the solution was then measured spectrophotometrically at a maximum wavelength of 231 nm using aliquots that had been appropriately diluted (Shimadzu UV-2450 spectrophotometer, Japan) [17, 18].

Preparation of ASD of APST by HME

The preparation of a solid dispersion of APST was conducted through an HME process. The most important critical process parameter (CPP) in HME is the complete melting of the active ingredient to form a molecular dispersion within the polymer matrix. The HME process involves several zones: feeding, mixing and conveying, kneading and melting, and finally, the die zone. Maintaining a lower temperature in the feeding and conveying zone facilitates effective blending and conveying of the mixture into the melt zone. Once the product enters the melting zone, a consistent temperature profile is maintained through the die.

Kollidon VA64 is used as the polymeric carrier for APST, also working as a plasticizer for the process. APST has a melting point of 157 °C, while the glass transition temperature of Kollidon VA64 is approximately 101 °C. Hence, for

Table 1 Operating ranges of key parameters in HME

HME process parameter	Parameter- Fixed/Variable	Range of process parameter
Screw diameter	Fixed	12 mm
Diameter ratio (Do/Di ratio)	Fixed	1.45
Feed rate (manual addition)	Variable	≈ 240 gm/h (4 gm/min)
Screw speed	Variable	55–100 rpm
Torque (%)	Variable	28–40%
Torque (Nm)	Variable	1.26–2.06
Chiller temperature	Fixed	7 °C

the HME process, the temperature range was selected from 40 °C to 160 °C. The screw speed impacts residence time, shearing force, and extruder torque. High speed increases the convection and thus the transport rate related to mixing, decreasing the residence time in the extruder [19]. Initially, according to the formulation design, the drug and polymer were sieved through a #30 ASTM mesh and thoroughly mixed using geometric mixing methods. Subsequently, the resulting physical mixtures underwent extrusion using a Twin Screw co-rotating hot melt extruder (Steer Engineering Model- Omicron 12 P). The extrusion processing conditions are mentioned in Table 1, and the temperature settings across different extrusion zones are detailed in Table 2. Following extrusion, the extrudates were subjected to milling using a mortar and pestle and then sieved through an ASTM #30 mesh. The sieved powder was subsequently weighed to achieve the desired drug load and encapsulated in hard gelatin capsules for further investigations.

To produce third-generation ASD, a physical blend of APST and polymer underwent further treatment. Initially, vitamin E TPGS was dissolved in acetone to prepare a solution. This solution was then added to the blend with continuous mixing [20]. When the wet mass was obtained, mixing was stopped, and the material was placed in a vacuum dryer at 40 °C for 2 h. After drying, the blend was passed through ASTM #25 mesh. The resulting physical mixture was then extruded through a hot-melt extruder.

Preliminary screening experiments were conducted prior to optimization trials. Table S1 presents the composition of these preliminary experiments, which aimed to ascertain the suitable ranges of drug: polymer and surfactant for inclusion in the final optimization studies.

Table 2 Temperatures across extrusion zones

Zone 1	Zone 2	Zone 3	Zone 4	Zone 5	Zone 6	Zone 7	Die Temp
Feed zone	Mixing and conveying zone	Mixing and conveying zone	Mixing and conveying zone	Kneading and melting zone	Kneading and melting zone	Kneading and melting zone	Die zone
40 °C	80 °C	110 °C	130 °C	150 °C	160 °C	160 °C	160 °C

Optimization of Formulation

Following a preliminary screening experiment, formulation optimization was carried out using a DoE approach. JMP 17.0 software was employed to select the appropriate set of experiments for optimizing the formulation. Response Surface Methodology (RSM) was then utilized to determine the final ratio of drug, polymer, and surfactant in the formulation. The formulation optimization was accomplished through the utilization of a central composite design (CCD), guided by the experimental suggestions provided by JMP 17.0 software. CCD is a statistical experimental design commonly applied in RSM. This design proves beneficial for constructing a second-order (quadratic) model for the response variable, eliminating the necessity for a complete three-level factorial experiment. CCD allows for the rapid estimation of first-order and second-order terms in the optimization process.

In this experimental setup, two independent variables were considered: the amount of Kollidon VA64 concentration (X1) and the amount of vitamin E TGPS (X2). Each factor was assigned high, low, and medium levels, represented by specific codes. The coding scheme followed a pattern where the first letter indicates the polymer level, while the second letter denotes the surfactant level. For instance, "0" signifies the medium level of both polymer and surfactant, "A" or "+" indicates the high level of polymer and surfactant, and "a" or "-" represents the low level of polymer and surfactant. The dependent variables under investigation were solubility in 1 h, 24 h, and dissolution in 15 min, 30 min, and 45 min.

Using the generalized response surface model and polynomial Eq. (4), the response surface behaviour was examined for the response function (y), as demonstrated.

$$Y_i = \beta_0 + \beta_1 x_1 + \beta_2 x_2 + \beta_{11} x_1^2 + \beta_{22} x_2^2 + \beta_{12} x_1 x_2 \qquad (4)$$

where y is the predicted response; β_0 is constant; $\beta_1 \beta_2$ are coefficient of regression for independent factor X1 and X2, $\beta_{11} \beta_{22} \beta_{12}$ are coefficient of regression for interaction effect.

$X1^2$ and $X2^2$ represents the curvature effect, $X1\,X2$ represent the interaction effect of input variables.

The analysis of variance (ANOVA) was used to determine the significance of the differences between the independent variables. For a visual representation of the factors' impact on responses, the prediction profiler was employed. To achieve the maximum response for dissolution and solubility, the maximum desirability function was utilized. A p-value of $< 0.05\%$ was considered to classify the impact as significant. Additionally, a good fit for the model was considered when the R^2 value exceeded 0.8, indicating a high level of correlation and reliability in representing the experimental data [21].

In Vitro Drug Release

In vitro drug release was assessed using a Distek dissolution apparatus. Formulations were encapsulated in gelatin capsules, each containing 20 mg of drug. Dissolution studies were conducted in 900 mL of 6.8 phosphate buffer dissolution media in USP-II paddle apparatus, rotating at 50 rpm, and maintained at a temperature of 37 °C ± 0.5 °C. At specified time intervals, aliquots of 7 mL were withdrawn from the dissolution media and replaced with an equivalent volume of fresh media to maintain sink conditions. The collected aliquots underwent filtration through a nylon filter (0.45 μm). The initial few mL of filtered aliquots were discarded. Samples were then subsequently analyzed using a UV apparatus at the wavelength of maximum absorption (λmax) of 231 nm.

DSC

The thermal properties of the APST; Kollidon VA64; vitamin E TPGS; APST and Kollidon VA64 in the ratios of 1:3 and 1:5 respectively; 1:5 APST + Kollidon VA64 + 2.5% vitamin TGPS; and 1:5 APST + Kollidon VA64 + 5% vitamin TGPS were evaluated using DSC (Mettler Toledo). Prior to analysis, the instrument was pre-calibrated using Zinc and Indium standards. The samples, as listed in Table S2, were scanned over a temperature range of 30 °C to 180 °C at a heating rate of 10 °C/min under a nitrogen atmosphere (40 mL/min). Each experiment utilized approximately 3 mg of the sample, which was placed in 40 μL crimped aluminium pans [22].

pXRD

The crystallinity of APST, its solid dispersion, and individual components were analyzed through pXRD studies. The diffraction patterns were generated using a PANalytical X'Pert PRO diffractometer equipped with a copper anode (Cu K radiation) operating at 40 kV voltage and 40 mA current. The scanning parameters included a step size of 0.02° and a scan speed of 0.01°/second, covering a 2θ range from 3° to 40° [22].

FTIR Spectroscopy

IR spectroscopic experiments were conducted using a Perkin Elmer FTIR spectrophotometer, model Spectrum One. The spectrum experiment covered a wavelength range from 4000 to 400 cm^{-1}. The FTIR spectra were instrumental in

understanding the interaction between Kollidon VA64 and APST in the resulting ASD [23].

Surface Morphology

The shape and surface morphology of the produced solid dispersions were investigated utilizing a scanning electron microscope (SEM) (Jeol, Model JSM-6010LA, Japan) [24]. Before microscopy analysis, all samples underwent platinum sputter-coating in argon treatment to enhance conductivity and minimize charging effects. The examination of the samples was carried out at 50X magnification.

Hygroscopicity Studies

To assess the moisture sensitivity of the produced ASD, DVS tests were conducted [25]. A known amount of sample was weighed and kept in the sample holder (DVS Advantage, Surface Measurement Systems Ltd., UK) in a chamber with controlled pressure and temperature. The change in mass was monitored at a variety of humidity levels in order to understand the effects of moisture. Testing was conducted for three hours at a constant temperature of 30 °C under different humidity conditions (0%, 30%, 60%, and 90%).

Stability Studies

The prepared ASD of APST was subjected to stability investigations in a stability chamber (Newtronics) with two temperature controls: 40 °C/75% RH and 25 °C/60% RH. Filled capsules of ASD, after being enclosed in closed high-density polyethylene (HDPE) containers, were placed in a stability chamber. Following a three-month duration, the samples were taken out of the stability chamber for analysis. To monitor changes in crystallinity compared to their initial stability, samples underwent pXRD and DSC examinations.

Table 3 Pharmacokinetic input parameters for in silico modelling

Parameters	Values
Molecular weight (gm/mol)	460.51[a]
pKa	10.88 [a]
Solubility (mg/mL) at pH 6.8	0.043[c]
Human permeability [Peff(cm/s $\times 10^4$)]	1.5[b]
Particle density (gm/mL)	1.2[b]
Diffusion coefficient (cm^2/s) $\times 10^5$	0.6[b]
Log P	1.8 [a]
Mean precipitation time (s)	900 [b]
CL/F L/h	11.6[c]
Oral dose (mg)	20[c]

[a]Predicted by ADMET predictor (Version 7.2.0.0, Simulations Plus, Inc., Lancaster, CA, USA)

[b]Default GastroPlus™

[c]Literature value

Additionally, dissolution tests were conducted on stability samples to detect any significant changes in dissolution behaviour.

GastroPlus Simulation

Physiologically based biopharmaceutics modeling (PBBM) and simulation of oral absorption profiles for APST were conducted using GastroPlus™ (version 9.0, Simulations Plus Inc., Lancaster, CA, USA). The ACAT model was employed to calculate the fraction of absorbed drug in the respective compartments of the intestine. Pharmacokinetic parameters like Cmax and AUC were estimated by software to understand rate and extent of absorption profile of APST, in which AUC was estimated by the linear trapezoidal linear interpolation method for both predicted and observed values. The input parameter values utilized in the modeling were extracted from the literature [14], supplemented by a few parameters obtained using the ADMET Predictor module of GastroPlus. The corresponding pharmacokinetic input parameters for in silico modelling are presented in Table 3. An initial PBBM model for plain APST drug was constructed and validated using an in vivo profile extracted from the literature. Some pharmacokinetic parameters were adjusted slightly to align with the observed in vivo human profile obtained from the literature. Prediction error was calculated to assess the accuracy of predicted pharmacokinetic values and validate the developed model.

Following the validation of the initial base model, dissolution data for both the solid dispersion formulation and plain drug were incorporated into the software to simulate absorption and determine their pharmacokinetic parameters. Using the dissolution data and the previously input modeling parameters, plasma drug concentration profiles were generated. The GastroPlus Population Estimates for Age-Related (PEAR™) Physiology Module was utilized for population modeling of both plain drug and solid dispersion formulations. A process flowchart, shown in Fig. S1, illustrates the modelling strategy employed in building the absorption model and conducting absorption simulations.

Results and Discussion

TGA

Thermogravimetric analysis is a method of thermal analysis in which the mass of a sample is measured over time as the temperature changes. As the sample is heated over time at increasing temperatures, there is a loss in the weight of the sample. This loss may be associated with the loss of moisture, solvent, or mass from the solid by vaporization

of the solid. TGA was carried out, and in Fig. 1, two distinct weight loss steps are illustrated. The first step, accounting for a weight loss of 1.016% (w/w), can be attributed to the loss of water/solvent. The second weight loss step commences at approximately 210 °C, with a weight loss of 1.636% (w/w). This second loss might be linked to the degradation of APST, indicating the breakdown of the compound [26]. Figure 1 provides a visual representation of the thermogram of APST, depicting its thermal behaviour and decomposition characteristics.

Determination of Thermodynamic Properties of APST

The Tg, also known as the critical molecular mobility area, is a crucial parameter to determine whether a glassy material will be strong or fragile [12]. Table 4 provides a summary of the thermodynamic characteristics of the crystalline and amorphous states of APST. Amorphous APST revealed a Tg of 76.05°C upon reheating. The ability of APST to transform into an amorphous state once the melt is supercooled is determined by its glass-forming ability (GFA). The GFA of a compound refers to its propensity to remain in an amorphous state without recrystallizing, which in turn provides insight into the stability of the compound. It is expressed as a ratio, Tg/Tm, where Tm is the melting temperature and Tg is the glass transition temperature. For optimal glass production, this ratio is higher than 0.7. From Fig. 2, the melting point of APST was determined to be 157°C, evident from a distinct single sharp endothermic peak with a corresponding Tg of 76.05°C. This yields a Tg to Tm ratio of 0.48, indicating that APST would be a borderline candidate for an ASD. Further, according to the literature, the rapid phase conversion and recrystallization of an ASD occur when there is a transition from the glass phase to the liquid phase at elevated temperatures above the Tg [27]. Following the 'Tg − 50°C' rule, it is recommended to store ASDs at temperatures at least 50 °C below their respective Tg [28]. If molecular mobility is ceased by mechanisms such as hydrogen bonding, the conversion from the amorphous state to the crystalline state can be prevented. The enthalpy of fusion (Hm), determined through peak integration, was found to be 88.56 J/gm. The sharp endothermic peak, indicating the melting point of crystalline APST, formed the basis for deriving several thermodynamic characteristics. Specifically, this peak facilitated the calculation of the fusion's entropy (Sm = Hm/Tm).

Hansen Solubility Parameter (HSP)

An established tool for estimating the solubility behaviour of a substance involves the concept of solubility parameters. Specifically, the HSP is derived from Van Krevlen's group
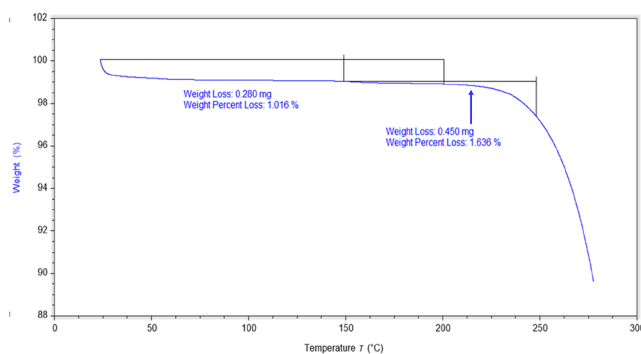

Fig. 1 TGA thermogram of APST

Table 4 Thermodynamic properties of APST

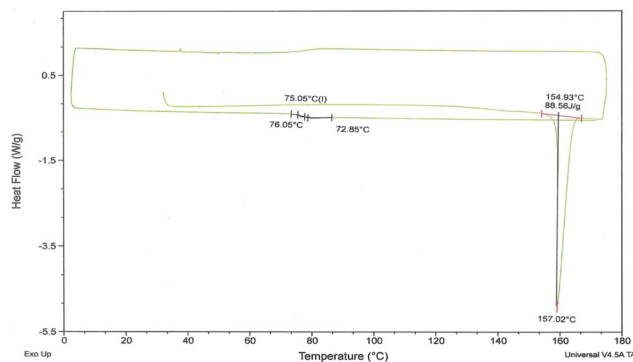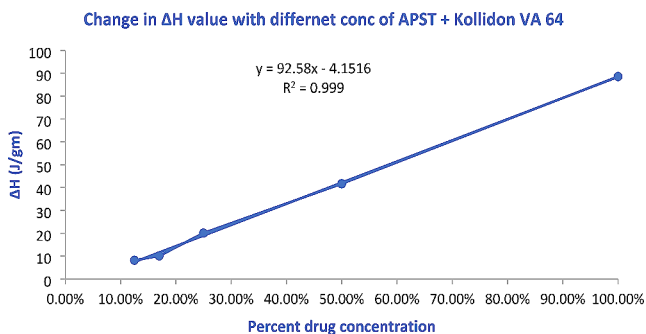| Thermodynamic property	Unit	Value
Melting temperature (Tm)	°C	157
Enthalpy of fusion (ΔHm)	J/gm	88.56
Entropy of fusion (ΔSm) ΔHm/Tm	J/gm/C	0.56
Glass transition temperature (Tg)	°C	76
Tm/Tg	-	2.06

Fig. 2 DSC thermogram of APST

contribution values. It accounts for the combined effects of dispersion forces, hydrogen bonding, and polar forces on the solubility of drugs within polymer matrices. These three parameters can be visualized as coordinates in a three-dimensional (3D) diagram, providing a useful illustration of the miscibility or solubility of different materials. The closer the coordinates of two substances are in this 3D space, the better their mutual solubility [29]. Furthermore, understanding solid-state solubility is crucial for determining appropriate drug loadings when creating stable solid dispersions. By strategically selecting carrier polymers based on the drug's molecular structure, formulation development can be streamlined. Polymeric carriers with structural similarities are more likely to form thermodynamically stable molecular dispersions, leading to an increased apparent solubility of the drug molecule.

An effective method to predict the miscibility of drugs and polymers involves utilizing the HSP. Solubility parameters

Table 5 Hanssen solubility parameters of APST, Kollidon VA64 calculated by using Van Krevlen's group contribution values

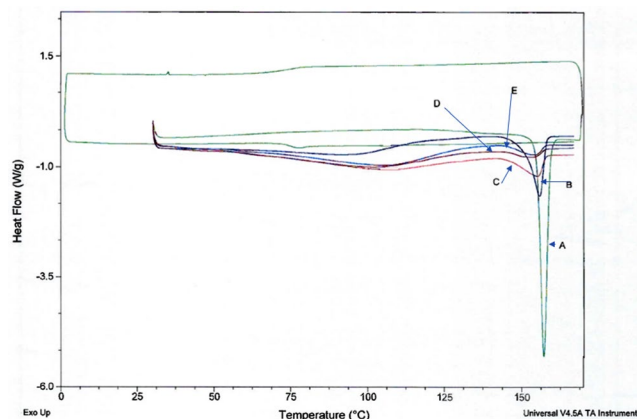| Contributing forces	Δd (dispersive forces)	Δp (polar forces)	Δh (hydrogen bonding forces)	δ (MPa1/2)$	Tg	ΔTg
APST	20.46	8.59	8.91	23.91	76**	-
Kollidon* VA64	19.4	9.7	9.6	23.72	101*	25
Difference	1.06	1.11	0.69	0.19		

* [13], $ Calculated from equation, ** Calculated from DSC by melt quenching method

Fig. 3 Change in ΔH value with different concentration of Kollidon VA 64

Fig. 4 the DSC overlay of APST with varying ratios of Kollidon VA64. **(A)** APST alone; APST combined with Kollidon VA64 at ratios of **(B)** 1:1, **(C)** 1:3, **(D)** 1:5, and **(E)** 1:7, respectively

for Kollidon VA64 [13] and APST [14] were determined using literature sources. Table 5 outlines individual solubility parameter values (δ) for APST and Kollidon VA64 based on the Van Krevlen group contribution approach. According to the standard solution theory "like dissolves like," when the difference in δ values (Δδ) between two components is less than 7 MPa$^{1/2}$, favorable interactions and a uniform phase are expected. Conversely, if the difference exceeds 10 MPa$^{1/2}$, unfavorable interactions and phase separation are likely. In adherence to this theory, when two solvents exhibit similar solubility parameters, they can be mixed in any ratio to form a uniform solution. Applying this principle, a miscible drug-polymer solid dispersion could be achieved by predicting close solubility characteristics between pharmaceuticals and polymers. Table 5 presents the solubility parameter differences between Kollidon VA64 and APST. Due to the smaller difference in the computed solubility parameters for APST and Kollidon VA64, it can be assumed that APST might be miscible with Kollidon VA64. Moreover, when the Tg values of components are comparable, more interactions are anticipated during the heating process, as the Tg signifies the temperature at which polymer chains become flexible. The Tg value for amorphous APST is 76 °C, whereas for Kollidon VA64, it is 101 °C, resulting in a small difference of 25 °C within the heating range suitable for the HME process to facilitate interactions between these two polymers [13].

F-H Interaction Parameter

There are many ways to measure solubility in the solid state of a drug in a polymer, both theoretically and practically,

based on various mechanisms, and one such mechanism is the enthalpy of fusion [18]. Theeuwes et al. calculated the drug solubility using the enthalpy of fusion, which is commonly defined as the heat required to change a substance from a solid to a liquid state without raising the temperature. This calculation was based on the assumption that the dissolved drug had no bearing on the endothermic event between the two components. So, by plotting the enthalpy of fusion on y axis and drug load on x axis, intercept on x axis will be the theoretical solubility of the drug within the polymer [30]. The enthalpy of fusion (ΔH) of APST with each concentration of polymer was recorded as shown in Fig. 3.

A linear correlation was obtained with an R^2 value of 0.99. The solubility of APST in the Kollidon VA64 polymer was found to be approximately 7% w/w. The lattice-based F-H theory has allowed for a thorough understanding of the miscibility amongst polymers. According to the F-H theory, there are two components to the free energy of mixing: an entropy component that consistently encourages mixing and the other enthalpy component that can aid in or obstruct mixing, based on the type and strength of the relationship between the two components. Here, the miscibility of the drug APST with Kollidon VA 64 was ascertained by means of the melting point depression method. This facilitated the determination of the F-H interaction factor (χ) using Nishi–Wang's modified F-H Eq. (2) [12].

Figure 4 displays the DSC overlay of APST with different ratios of Kollidon VA64. Table 6 summarizes the

Table 6 Thermodynamic output of DSC of APST and Kollidon VA64 mixture

Sr. no.	APST: Kollidon VA64 ratio	APST	Kollidon VA64	Melting point (°C)	Melting point (K)	Delta H (J/gm)
1	0	100	0	157.02	430.17	88.56
2	1:1	50	50	155.70	428.85	41.65
3	1:3	25	75	155.17	428.32	20.08
4	1:5	17	83	154.24	427.39	10.08
5	1:7	12.5	87.5	153.63	426.78	8.198
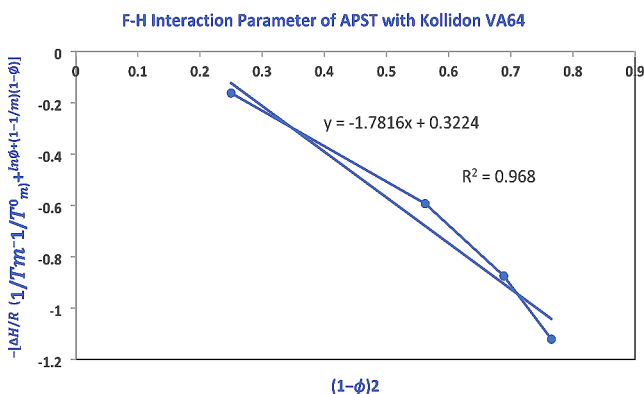
Fig. 5 F-H interaction parameter of APST with Kollidon VA 64

thermodynamic output obtained from the DSC analysis of the APST and Kollidon VA64 mixture.

The value for T_{0m} or melting point of pure drug was obtained to be 430.17 K, R was considered to be 8.321 J/K/mol, ΔH to be 40781.88 J/mol (Mol wt $\times \Delta H$). APST exhibits a molecular weight of 460.5 gm/mol, a molecular volume of 328.93 cm³/mol, a density of 1.4 gm/cm³ [14], and a melting point of 430.17 K whereas Kollidon VA64 displays a molecular weight of 50,000 gm/mol, molecular volume of 43,103 cm³/mol, density of 1.16 gm/cm³, and a melting point of 413.15 K.

According to the F-H theory, total, partial, or zero miscibility can be discovered at a given temperature with an interaction parameter of > 0 (very poor miscibility), 0 (poor miscibility), or < 0 (strong miscibility) [31, 32]. A negative interaction parameter between the two components (in this case, drug, and polymer) indicates a stronger-than-average attraction between a drug-polymer system and a drug-drug system. Therefore, in this situation, drug molecules prefer to engage with polymer segments over other drug molecules. The value also becomes more negative when these interactions are very strong. Conversely, situations wherein drug molecules prefer to be near other drug molecules and polymer molecules like to be near other polymer molecules rather than combining with one another are indicated by a positive interaction value. As observed in the graph, the slope of the equation was negative, and the R^2 was 0.968, suggesting excellent miscibility of APST with Kollidon VA64 (Fig. 5).

Phase Solubility Studies

The solubility of APST in water was determined to be 7.551 ± 1.2 µg/mL. Additionally, the saturation solubility of APST in copovidone and hypromellose (5 cps) was evaluated. Furthermore, the solubility in surfactants, including poloxamer and vitamin E TPGS, was also investigated, as summarized in Table S3. Solutions containing polymers and surfactants in concentrations ranging from 0 to 10% w/w were analyzed. The phase solubility curves for both the polymer and surfactant can be found in Fig. 6A and B, respectively.

In an A_L-type phase solubility profile, one drug molecule forms a compound with one ligand molecule, characterized by the association constant K1:1, indicating a linear relationship. Kollidon VA64 exhibited an A_L-type phase solubility profile described by the equation $y = 0.1151x - 0.0068$, with a high correlation coefficient ($R^2 = 0.977$) (Fig. 6A). With HPMC, conversely, the solubility profile exhibited an A_N-type pattern, with no evident enhancement in solubility observed. Further, the solubility of the drug increased with the rise in surfactant concentration. Among the two surfactants evaluated, vitamin E TGPS exhibited a linear relationship, as indicated by the equation $y = 0.087x + 0.0279$ and a high correlation coefficient ($R^2 = 0.999$) (Fig. 6B). This suggested that the data adhered to an A_L-type phase solubility curve. The surfactant properties of vitamin E TGPS likely contributed to improved dissolution of the drug particles by enhancing their wettability. Beyond a 1% concentration, an abrupt increase in solubility may be attributed to increased solubilization following the critical micelle concentration. Thus, Kollidon VA64 was selected as the polymer, and vitamin E TPGS was chosen as the surfactant based on phase solubility experiments to formulate ASD using the HME technique.

Characterization of ASD of APST by HME

Various combinations of the drug and polymer were prepared with different surfactants: SD1, without surfactant in a 1:1 ratio; SD2, with poloxamer 2.5%w/w as surfactant in a 1:1 ratio; SD3, with vitamin E TPGS (1.66% w/w) as surfactant in a 1:2 ratio; SD4, with vitamin E TPGS (2.5% w/w) as surfactant in a 1:5 ratio; and SD5, with vitamin E TPGS (5%

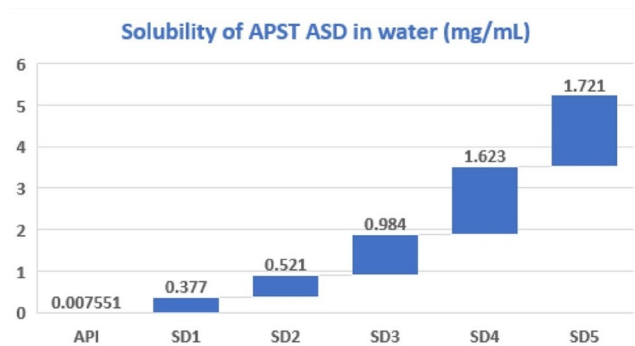**Fig. 6** Phase solubility studies of APST with various polymers and surfactants

A Solubility of APST in varying polymer concentration

$y = 0.1151x - 0.0068$
$R^2 = 0.977$

$y = 0.0015x + 0.0211$
$R^2 = 0.9915$

Solubility (mcg/mL) vs Concentration of polymer (w/v)

— VA 64 solubility   — HPMC -solubility

B Solubility of APST in varying surfactant concentration

$y = 0.0867x + 0.0279$
$R^2 = 0.999$

$y = 0.0048x + 0.0029$
$R^2 = 0.9762$

Solubility (mcg/mL) vs Concentration of surfactant (w/w)

— TPGS solubility   — P-188 -solubility

Solubility of APST ASD in water (mg/mL)

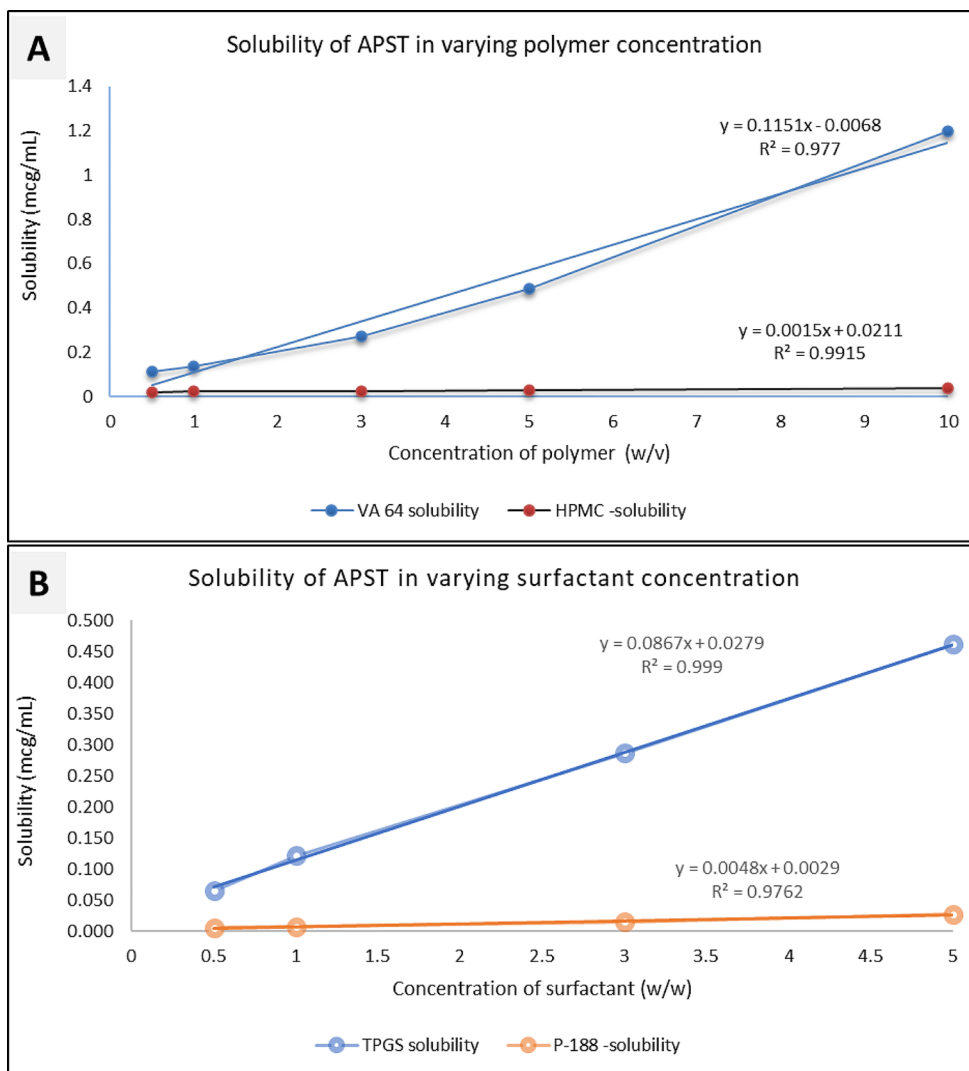API 0.007551, SD1 0.377, SD2 0.521, SD3 0.984, SD4 1.623, SD5 1.721

Fig. 7 Screening experiment results for solubility enhancement in SD1 to SD5 formulation

w/w) as surfactant in a 1:5 ratio. Solubility enhancement results are detailed in Table S4, while the screening experiment outcomes for solubility enhancement in SD1 to SD5 formulations are depicted in Fig. 7. Furthermore, dissolution studies of these formulations (SD1, SD2, SD3, SD4, and SD5) were conducted in phosphate buffer 6.8, with the results presented in Fig. S2.

The solubility increased significantly with higher concentrations of Kollidon VA64, peaking at approximately 227 times. Moreover, preliminary experiments indicated that the solubility and dissolution of APST increased with higher concentrations of both polymer and surfactant. Therefore, DoE studies were employed to optimize the formulation.

DoE for Optimization of Formulation

After preliminary screening experiments, the formulation was further optimized to arrive at optimum levels of polymer and surfactant ratio. Using a two-factor, three-level design, third generation solid dispersions of APST were prepared. This design was effective for constructing models of second-order polynomials and determining quadratic response surfaces. Table 7 represents the experiments

Table 7 Design matrix for optimization and the observed outcomes

| Pattern	Factors		Responses				
	Kollidon VA 64 conc.	Vitamin E TPGS conc.	Solubility (mg/mL) 1 h	Solubility (mg/mL) 24 h	%DR 15 min	%DR 30 min	%DR 45 min
0	2.5	2.5	1.21	1.242	28.3	46.3	64.3
A0	5	2.5	1.623	1.712	93.9	94	94
0	2.5	2.5	1.21	1.242	28.3	46.3	64.3
−+	0	5	0.091	0.093	14.5	28.3	42.4
−−	0	0	0.007551	0.007551	7	28.1	28.7
++	5	5	1.721	1.811	93.2	93.9	93.3
0 A	2.5	5	1.321	1.356	34.4	56.7	74.2
a0	0	2.5	0.087	0.092	16.2	28.4	42
+−	5	0	1.348	1.391	60.4	75.3	90
0a	2.5	0	0.1078	0.1084	18.4	30.5	46
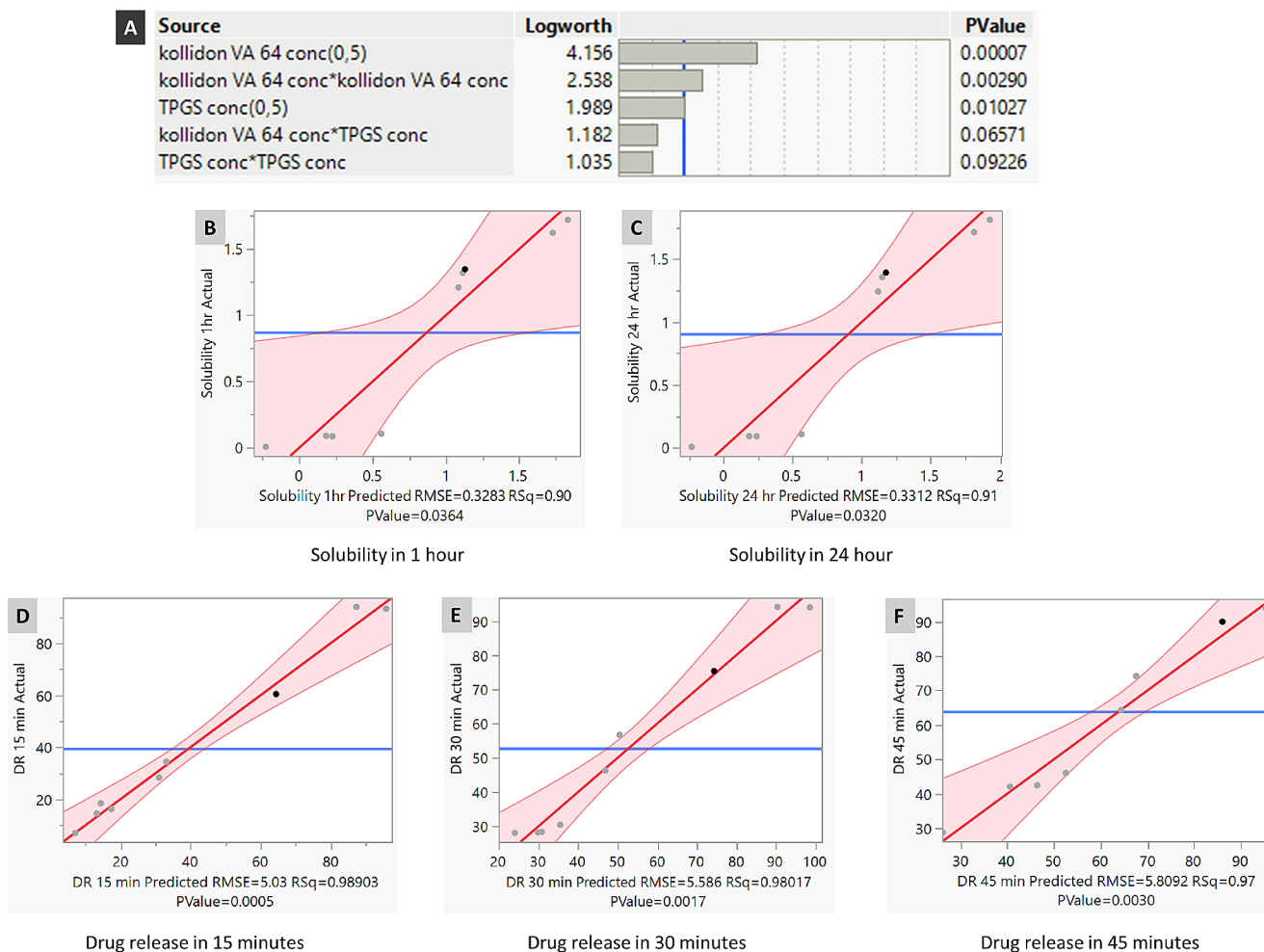
Fig. 8 Actual vs. predicted profile along with R^2 value and p value

suggested by the software and the experimental outcomes of the experiments.

Figure 8A highlights the significance of various factors affecting solubility and dissolution, with Kollidon VA64 concentration emerging as the most crucial factor. Further, an effective correlation between input variables and the

output response is highlighted by an R^2 value exceeding 0.90 for solubility and dissolution parameters, suggesting the model's significance in comparison to the predicted profile (Fig. 8B-F). Additionally, a significant relationship between the input variables (solubility within 1 h, 24 h, and dissolution rate within 15 min) and the output response was

confirmed by a p-value below 0.05, further affirming the model's significance. Table S5 and Table S6 shows parameter estimates and effect summary respectively. Parameter estimates (also called coefficients) are the change in the response associated with a one-unit change of the predictor, all other predictors being held constant. Parameter estimates shows estimate of parameter in linear model and t test for hypothesis that each parameter is zero. The effect test for a given effect tests the null hypothesis that all parameters associated with that effect are zero. The effects table uses a F-test against a zero change in the model sum of squares. Prob > F value, or p-value, in an effect test measures the likelihood of obtaining an F ratio as large as the observed one, assuming all parameters except the intercept are zero. A small Prob > F value indicates that the observed F ratio is unlikely, and is considered evidence of at least one significant effect in the model [33]. Data shows that the most significant factor affecting the solubility and dissolution is concentration of Kollidon VA64. Other factor that is impacting solubility and dissolution is concentration of vitamin E TPGS, however p values are $p > 0.05$ but less than 0.1.
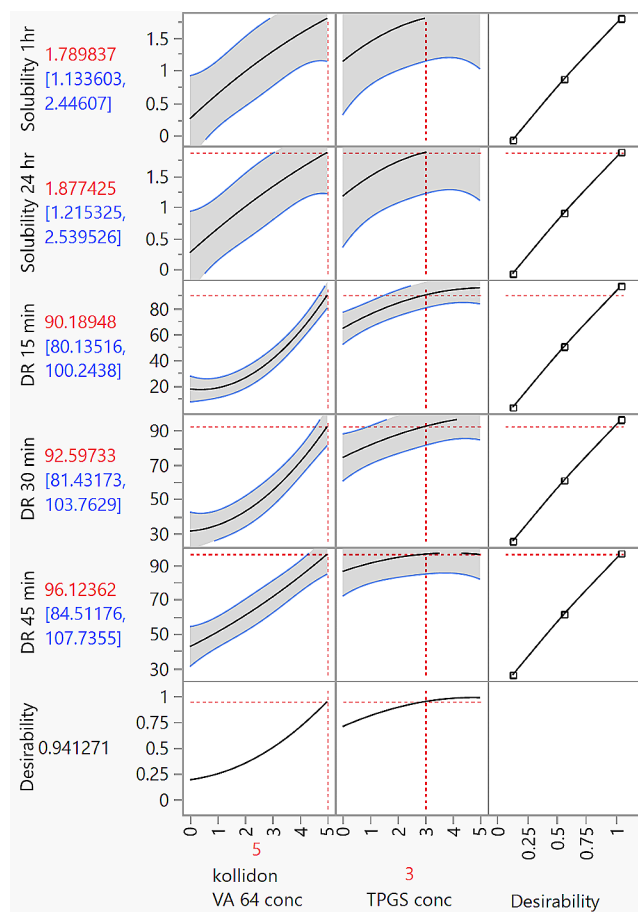

Fig. 9 Prediction profiler of APST with Kollidon VA64 and vitamin E TPGS

Prediction Profiler

With the objective of achieving maximum desirability, the formulation underwent further optimization to attain optimal levels of input factors. The maximum desirability function is depicted in Fig. 9. The prediction profiler (Fig. 9) illustrates the impact of changing the concentrations of Kollidon VA64 and vitamin E TPGS on solubility and dissolution. The formulation was further optimized to achieve maximum desirability. The best optimized formulation, yielding maximum desirability, consists of a 1:5 ratio of APST and Kollidon VA64 with the addition of 3% vitamin E TPGS surfactant. A linear increase in solubility and dissolution was observed with the increase in the concentration of Kollidon VA64. However, with vitamin E TPGS, no significant increase in solubility or dissolution was observed after reaching 3% w/w of vitamin E TPGS.

Additional 3D surface plots were generated using JMP-17.0. A surface plot presents 3D data, where one or more dependent variables are depicted by a smooth surface. Fig. S3 displays the relationship between the concentration of Kollidon VA64 and vitamin E TGPS and their impact on solubility and dissolution. Analysis of the 3D graphs revealed that beyond a concentration of 3% of vitamin E TPGS, there was no significant increase in dissolution and solubility.

DSC Studies

DSC measurements were carried out in order to understand the thermal behaviour and change in crystallinity of the developed solid dispersions of APST. As depicted in Fig. 10, the endothermic melting peaks were observed at 157 °C for APST, 40 °C for vitamin E TPGS, and Kollidon VA64 displayed a broader endothermic peak at 94 °C. The solid dispersion thermogram revealed the disappearance of crystalline APST peaks, indicating a successful conversion from crystalline to amorphous form for APST. The amorphization process was facilitated by the interaction between APST and the carrier. Additionally, the absence of endothermic peaks, even in the presence of the surfactant vitamin E TPGS, indicated that the amorphicity of the produced ASD remained unaffected by the addition of the surfactant.

pXRD

Due to its outstanding capability to produce fingerprints and quantitative analysis of compounds, pXRD has been the technique of choice to characterize solid dispersions in the pharmaceutical industry [34]. pXRD was performed to illuminate the crystalline state of the samples. Figure 11 displays an overlay of the pXRD data for individual components, their respective mixtures, and the developed ASD.

Fig. 10 DSC thermogram of
A=APST; **B**=Vitamin E TPGS;
C=Kollidon VA64; **D**=1:3
APST+Kollidon VA64; **E**=1:5
APST+Kollidon VA64; **F**=1:5
APST+Kollidon VA64+2.5%
vitamin TGPS; **G**=1:5
APST+Kollidon VA64+5%
vitamin TGPS

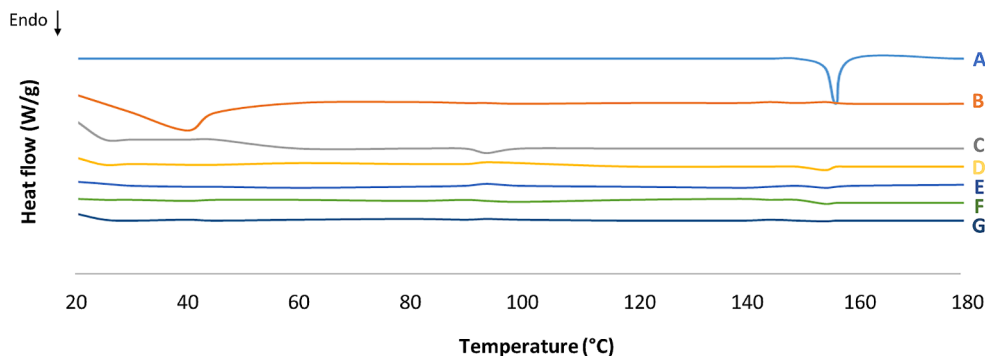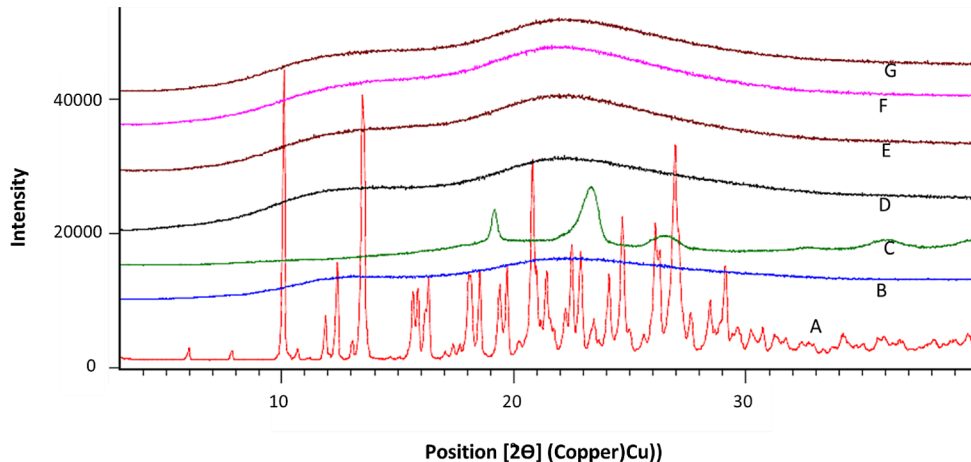**Fig. 11** XRD overlay of
various combinations, **A**=APST;
B=Kollidon VA64; **C**=Vitamin
E TPGS; **D**=1:3 APST+Kolli-
don VA64; **E**=1:5 APST+Kolli-
don VA64; **F**=1:5 APST+Kolli-
don VA64+2.5% vitamin
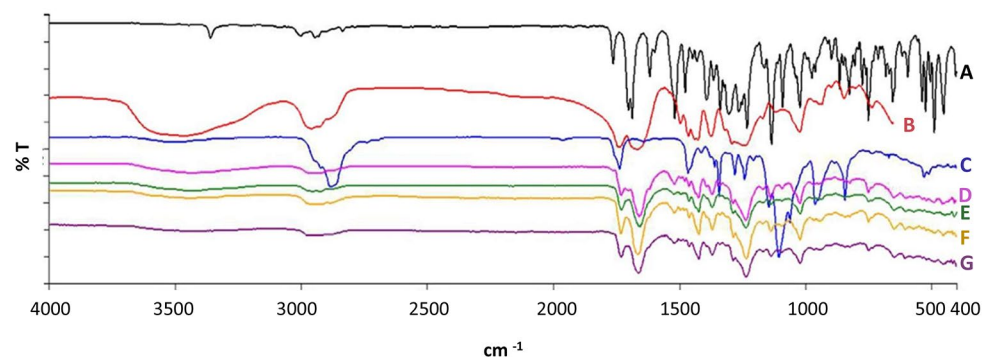TGPS; **G**=1:5 APST+Kollidon
VA64+5% vitamin TGPS

Fig. 12 FTIR overlay of
A=APST; **B**=Kollidon VA64;
C=Vitamin E TPGS; **D**=1:3
APST+Kollidon VA64; **E**=1:5
APST+Kollidon VA64; **F**=1:5
APST+Kollidon VA64+2.5%
vitamin TGPS; **G**=1:5
APST+Kollidon VA64+5%
vitamin TGPS

Sharp multiple peaks were visible in the X-ray diffracto-
grams of APST, indicating its crystalline nature. The pXRD
pattern of the APST exhibited characteristic peaks at diffrac-
tion angles (2θ) of 10.68°, 12.40°, 13.55°, 15.86°, 17.66°,
18.54°, 19.71°, 21.73°, 22.94°, 23.65°, 24.99°, 25.59°,
27.63°, 28.86°, 31.74°, 37.45°, and 39.56°, whereas vita-
min E TPGS showed its characteristic diffraction peaks at
2θ values of 19.2° and 23.4°. The pXRD pattern of Kollidon
VA64 did not exhibit any crystalline peaks due to its amor-
phous nature. In the pXRD diffractogram of the solid dis-
persion, APST appeared to have been transformed into an
amorphous form, as it did not display any distinctive peaks
of either vitamin E TPGS or APST [35, 36].

FTIR Studies

In the FTIR spectra (Fig. 12), a distinct peak at 3363 cm^{-1}
was observed, attributed to NH stretching in the pure APST
spectra. The peak at 1763.68 cm^{-1} corresponds to the aro-
matic -C=O ketone stretching vibration, while the peak
at 3003.95 cm^{-1} arises from the aromatic benzene ring
C-H stretching, and the peak at 1687.2 cm^{-1} is assigned
to the -C=O amide stretching. Additionally, the peak at
2946.8 cm^{-1} is linked to aliphatic C-H stretching. Com-
paring these findings with previously reported IR [37–39]
reveals matching peaks for APST, Kollidon VA64, and
vitamin E TPGS. Interestingly, peaks at 3003.95 cm^{-1}
(aromatic C=O ketone stretching) and 2496.8 cm^{-1} (C-H

Table 8 Solubility enhancement of APST formulations with various vitamin E TPGS concentrations

Formulation	Solubility 1 h (mg/mL)	Solubility 24 h (mg/mL)	Folds increase in solubility in 1 h	Folds increase in solubility in 24 h
Apremilast	0.007551	0.007551		
APST + Kollidon VA64 1:5 with 2.5% vitamin E TPGS	1.623	1.712	215-fold	227-fold
APST + Kollidon VA64 1:5 with 5% vitamin E TPGS	1.721	1.811	228-fold	240-fold
APST + Kollidon VA64 1:5 with 3% vitamin E TPGS (As predicted from DoE)	1.789	1.877	237-fold	248-fold

Fig. 13 Dissolution of APST with Kollidon VA64 and with/without vitamin E TPGS

Dissolution of APST ASD in 6.8 phosphate buffer 900 mL/50 rpm/USP-II
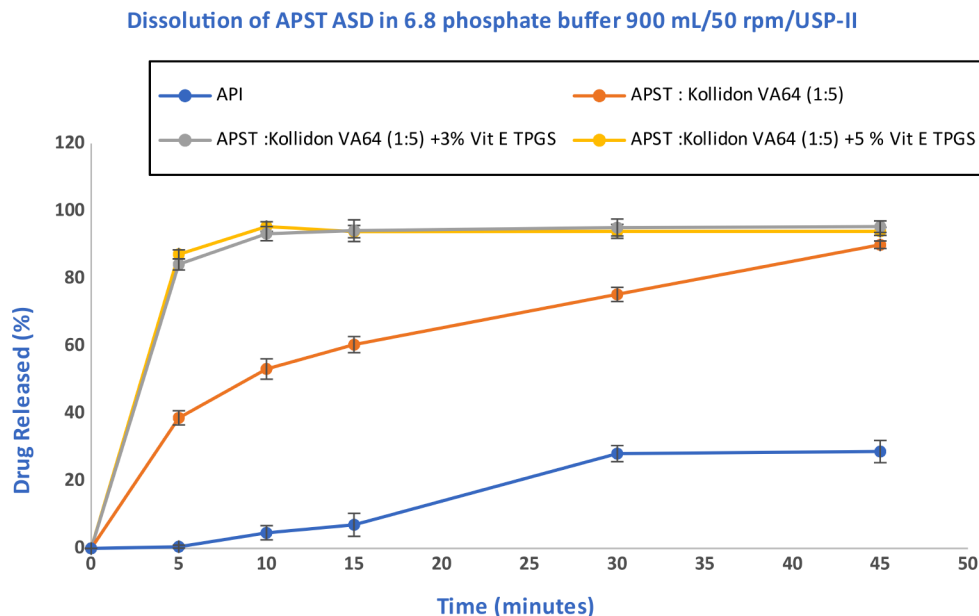
stretching) are absent in extrudates. In solid dispersion, there was a shift in peaks: from 1763.68 cm^{-1} to 1731.94 cm^{-1} and 1732 cm^{-1} for aromatic C=O ketone stretching, and from 1687 cm^{-1} to 1662.34 cm^{-1} and 1663.79 cm^{-1} for C=O amide stretching. Moreover, the NH stretching peak at 3363 cm^{-1} broadened and shifted to 3445.74 cm^{-1} in APST: Kollidon VA 64 (1:5) + 2.5%/5% TPGS, indicating possible hydrogen bonding between the drug and carrier, thereby enhancing solubility and dissolution. Such possible interaction might be due to a possible interaction between imino group of APST and carboxyl group of vitamin E TGPS. Such an interaction between apremilast and vitamin E TGPS is also reported by Yang et al. [23].

Solubility and In Vitro Drug Release Study

According to the DoE, no statistically significant difference was observed in the dissolution of APST + Kollidon VA64 formulations containing 2.5% and 5% vitamin E TGPS. Additionally, analysis of solubility data, as well as FTIR, DSC, and XRD data, revealed comparable results between formulations with 2.5% and 5% vitamin E TGPS. From

the DoE studies, it was found that the formulation with the highest desirability was achieved at the 3% level of vitamin E TGPS. Consequently, the final formulation was prepared using APST + polymer (1:5) with 3% vitamin E TGPS.

The solubility of pure APST was 0.007551 mg/mL, while the final ASD exhibited approximately a 237–248 fold increase in solubility. Table 8 illustrates the significant increase in solubility of APST formulations over 1 and 24 h, with varying concentrations of vitamin E TPGS in combination with APST and Kollidon VA64. For further investigation into the translation of solubility into increased dissolution rates, in vitro dissolution studies were conducted.

The in vitro drug release of the final formulation, compared to the pure drug and other combinations, is presented in Fig. 13. In the case of ASD, drug release experiments were conducted in 6.8 phosphate buffer without the addition of surfactant to the media. During the initial development trials, dissolution was conducted in both 0.1 N HCl and 6.8 buffer conditions. Similar dissolution profiles were observed in both conditions. Therefore, to mimic biological conditions where the drug remains for an extended period, 6.8 phosphate buffer was selected. Dissolution in 6.8 phosphate

buffer media without the presence of surfactant demonstrated an increase in dissolution. APST-ASD formulations showed a significant increase in dissolution compared to pure APST, indicating the effectiveness of ASD in enhancing APST dissolution. Notably, APST-ASD achieved nearly complete release within 45 min, regardless of the presence or absence of vitamin E TGPS.

Morphological Examination

SEM images of pure APST and APST solid dispersions at various magnifications are depicted in Fig. 14. The surface of pure APST appeared coarse (Fig. 14A) when compared to the solid dispersion. While SEM images of the formulation of APST with Kollidon VA64 and vitamin E TPGS (Fig. 14B) exhibited a smooth, uniform, and continuous surface; pure APST displayed finely agglomerated particles. This finding suggests that the drug particles were evenly distributed throughout the polymer matrix without any signs of drug, polymer, or surfactant phase separation. Similar findings have been reported in the literature, where SEM images were employed as proof to demonstrate that Alectinib does not crystallize from the generated solid dispersion [45].

Hygroscopicity Studies

ASD are extremely unstable with moisture because moisture can reduce the Tg, which increases molecular mobility and causes drug crystallization [25]. The rate at which a sample absorbs water can be measured using the gravimetric method known as DVS. The water uptake of the compound signifies its level of hygroscopicity. Hygroscopicity is highly relevant in the evaluation of storage conditions and general stability. A drug may change from its amorphous state back to its crystalline form when exposed to water. During processing or storage, ASD have a propensity to crystallize into a stable crystalline state, altering their physicochemical properties. The DVS isotherm of the third-generation solid dispersion of APST with Kollidon VA64 1:5 and 3% vitamin E TPGS is shown in Fig. S4. The moisture uptake was approximately 2.2% at 50% RH and 4.7% at 75% RH. This uptake was significantly lower than what was documented for pure polymer in the literature [40]. DVS analysis demonstrated that, due to the possible hydrogen bonding between APST and Kollidon VA64, the water uptake by the solid dispersions of APST with Kollidon VA64 and vitamin E TPGS was less likely.

Stability Studies for Final Formulation

At higher temperatures and humidity conditions, there may be an increase in molecular mobility and plasticization of material, which can convert material back to amorphous material to crystalline material [41]. So, the final formulation (1:5 APST:Kollidon VA64 + 3% vitamin TGPS) was evaluated with respect to the accelerated (ACC 40 ± 2 °C, 75% $\pm 5\%$ RH) and controlled (CRT 25 ± 2 °C, 60% $\pm 5\%$ R) conditions. pXRD and dissolution were two techniques used to assess any change in stability. Samples were evaluated for 3 months in ACC and CRT conditions. Findings revealed that there was no change in pXRD pattern when compared to the initial 3 months of ACC and CRT conditions, indicating that the amorphous form is maintained in samples (Fig. 15A). The dissolution profiles (Fig. 15B) remained consistent before and after the evaluation period, indicating the stability of the prepared ASD.

GastroPlus Simulation Results

GastroPlus™ (version 9.0, Simulations Plus Inc., Lancaster, CA, USA) was employed to carry out PBBM modelling and simulate oral absorption profiles for APST (Fig. S5 (A, i)).
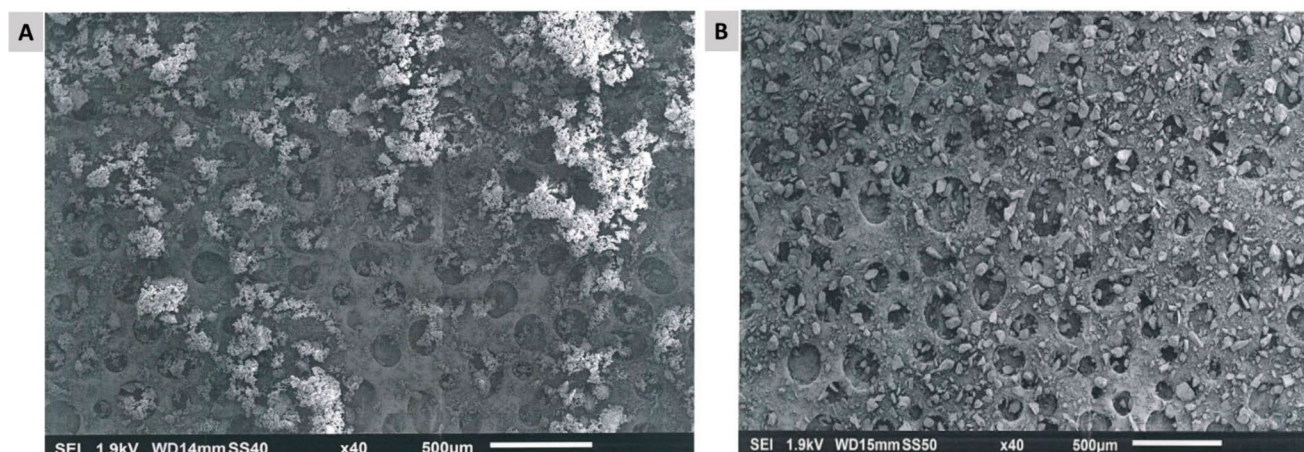

Fig. 14 SEM image of **(A)** Pure API, **(B)** ASD with 1:5 ratio of APST with KollidonVA64 and 3% vitamin TPGS (Scale bar: 500 μm)

Fig. 15 **(A)** pXRD pattern and **(B)** Dissolution profiles of 1:5 APST + Kollidon VA64 + 3% vitamin TGPS at various stability conditions
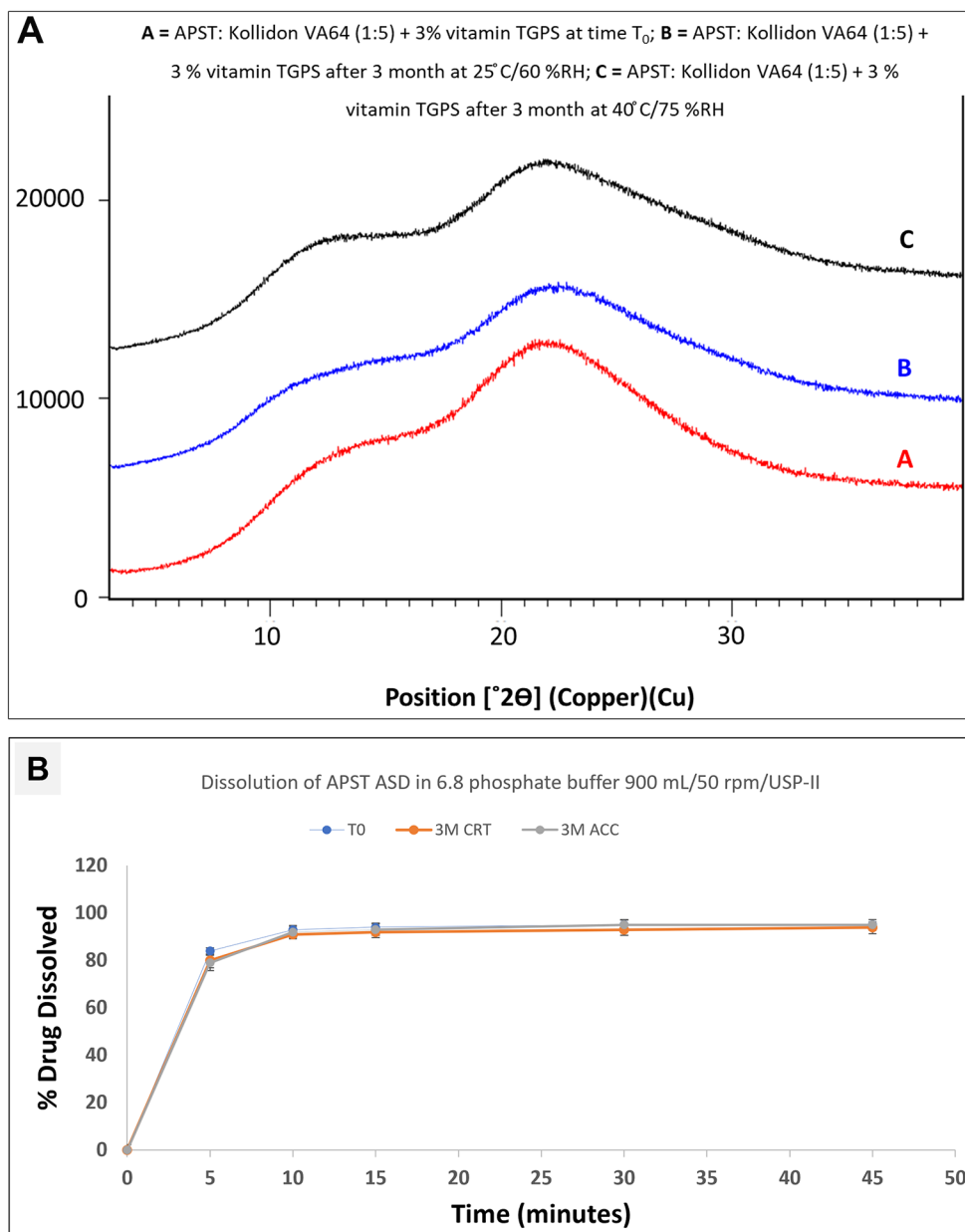

Table 9 Observed vs. predicted pharmacokinetics parameters

Result	Observed	Simulated	%PE error
Cmax (ng/mL)	168	170.1	1.25
AUC 0-t (ng-h/mL)	1809	1797.4	-0.64

The ACAT model was utilized to compute the fraction of absorbed drug in the respective compartments of the intestine. A comprehensive modeling technique was employed sequentially to learn the enhanced rate and extent of absorption and bioavailability associated with APST solid dispersion formulations, with in vitro dissolution generated at pH 6.8. Initially, a PBBM was developed for the plain APST, and its predictions were validated by comparing them to concentration-time profiles published in relevant literature for the plain APST. Specifics on pharmacokinetic parameters, encompassing both observed and predicted values, are provided in Table 9. The model demonstrates suitability for further runs and can be considered validated, with a prediction error of less than 10%. The simulation graphs for APST + Kollidon VA64 (1:5) and APST + Kollidon VA64 (1:5) with 3% vitamin E TPGS are presented in Fig. S5 (A, ii) and Fig. S5 (A, iii), respectively.

The same model was used to simulate and forecast in vivo profiles for the F-I (APST + Kollidon VA64 (1:5)) and F-II (APST + Kollidon VA64 (1:5) with 3% vitamin E TPGS), which were produced using the HME technique after the PBBM for the plain APST drug was developed and validated. The in vitro dissolution data for the F-I and

Table 10 Simulated pharmacokinetic parameters of ASD formulations

Result	F-I Simulated	F-II Simulated
Cmax (µg/mL)	0.465	0.482
AUC 0-t (µg-h/mL)	2.874	3.039

F-II formulations served as the basis for this simulation. Table 10 presents the simulated pharmacokinetic characteristics of ASDs.

Additionally, population modeling was done using a sample of 25 participants using the default physiological settings in GastroPlus for both the drug and formulations F-I and F-II. Fig. S5 (B) shows the population modeling findings for the pure drug, APST with Kollidon VA 64 (1:5), and APST: Kollidon VA64 (1:5)+3% vitamin E TPGS. Table 11 displays the results, which were in accordance with the model setting.

Population modeling results revealed a notable enhancement in the Cmax and AUC for both F-I and F-II compared to the plain drug when considering solid dispersion with polymers. Particularly, F-II demonstrated superior absorption and PK parameters (Cmax and AUC) compared to F-I and the plain drug, aligning consistently with the dissolution outcomes of the drug.

Conclusion

The successful manufacturing of an amorphous Apremilast solid dispersion using the HME technique was achieved. Phase solubility studies were conducted to evaluate surfactants for the third-generation ASD, with findings indicating that vitamin E TPGS displayed superior efficacy in enhancing drug solubility and dissolution. Vitamin E TPGS has been identified as a CYP3A4 inhibitor, the enzyme responsible for APST metabolism. Subsequently, based on phase solubility studies, Kollidon VA64 (copovidone) was selected as the polymer for the extrusion process. The utilization of Kollidon VA64 demonstrated an increase in solubility with increasing concentration. Notably, Apremilast combined with Kollidon VA64 in a 1:5 ratio exhibited the highest solubility and dissolution enhancement among all ratios examined. Additionally, the potential of vitamin E TPGS to further enhance APST solubility was evaluated. The developed formulation notably enhanced the drug's

solubility and dissolution, yielding a stable amorphous solid APST dispersion. DoE studies revealed that vitamin E TPGS at 3% further improved dissolution. The combination of polymer and surfactant enhanced wettability, while the drug's amorphous form, as confirmed by DSC and pXRD, contributed to enhanced dissolution. Moreover, SEM was employed to assess the generated ASDs, revealing uniformly distributed drug particles within a matrix of carriers. DVS studies confirmed minimum moisture uptake by prepared solid dispersion, indicating the stability of prepared ASD. Stability studies demonstrated that the formulation remained stable for up to three months under ACC and CRT conditions, as evidenced by both pXRD and solubility analysis. Results indicated the stability of the ASD for up to three months under accelerated conditions, suggesting its potential scalability for industrial applications. The combination of polymers and surfactants could increase wettability, with vitamin E TPGS reported as a permeability enhancer capable of further promoting absorption. Additionally, vitamin E TPGS, known to exhibit the ability to inhibit P-gp, might lead to a potential increase in the drug's bioavailability. The in silico GastroPlus simulations demonstrated an enhanced rate and extent of absorption compared to the pure drug. In conclusion, this study successfully demonstrates the development of a third-generation ASD of APST, significantly improving its solubility and pharmacokinetic parameters, and showcasing promise for industrial-scale production.

Table 11 Simulated population pharmacokinetic parameters

Result	Cmax (µg/mL)			AUC (µg.h/mL)		
	Plain	F-I	F-II	Plain	F-I	F-II
Mean	0.163	0.402	0.472	1.774	2.392	3.321
CV%	21.5	28.9	30.9	31.2	32.5	41.4
Min	0.111	0.210	0.216	0.923	1.182	1.051
Max	0.254	0.652	0.814	3.077	4.318	6.779
Geomean	0.159	0.385	0.449	1.689	2.2781	3.024

Author Contributions AF- Study conception and design; data collection; analysis and interpretation of results, draft manuscript preparation. AJ- Data collection; draft manuscript preparation, analysis and interpretation of results. PN- Study conception and design, analysis and interpretation of results. DR- Analysis and interpretation of results, draft manuscript preparation. DB- Analysis and interpretation of results, draft manuscript preparation. All authors reviewed the results and approved the final version of the manuscript.

Declarations

Ethical Approval Not applicable.

Consent Not applicable.

Competing Interests The authors declare no competing interests.

References

1. Kalepu S, Nekkanti V. Insoluble drug delivery strategies: review of recent advances and business prospects. Acta Pharm Sin B. 2015;5(5):442–53.
2. Kallakunta VR, Sarabu S, Bandari S, Batra A, Bi V, Durig T, et al. Stable amorphous solid dispersions of fenofibrate using hot melt extrusion technology: Effect of formulation and process parameters for a low glass transition temperature drug. J Drug Deliv Sci Technol. 2020;58:101395.
3. Patil H, Tiwari RV, Repka MA. Hot-melt extrusion: from theory to application in Pharmaceutical Formulation. AAPS PharmSciTech. 2016;17(1):20–42.
4. Repka MA, Shah S, Lu J, Maddineni S, Morott J, Patwardhan K, et al. Melt extrusion: process to product. Expert Opin Drug Deliv. 2012;9(1):105–25.
5. Lee JY, Kang WS, Piao J, Yoon IS, Kim DD, Cho HJ. Soluplus®/TPGSGS-based solid dispersions prepared by hot-melt extrusion equipped with twin-screw systems for enhancing oral bioavailability of valsartan. Drug Des Devel Ther. 2015;9:2745–56.
6. Tekade AR, Yadav JN. A review on solid dispersion and carriers used therein for solubility enhancement of poorly water soluble drugs. Adv Pharm Bull. 2020;10(3):359–69.
7. Tran P, Pyo YC, Kim DH, Lee SE, Kim JK, Park JS. Overview of the manufacturing methods of solid dispersion technology for improving the solubility of poorly water-soluble drugs and application to anticancer drugs. Pharmaceutics. 2019;11(3):132.
8. Hallouard F, Mehenni L, Lahiani-Skiba M, Anouar Y, Skiba M. Solid dispersions for oral administration: an overview of the methods for their Preparation. Curr Pharm Des. 2016;22(32):4942–58.
9. Wang FY, Zhang Q, Zhang Z, Gong X, Wang JR, Mei X. Solid-state characterization and solubility enhancement of apremilast drug–drug cocrystals. CrystEngComm. 2018;20(39):5945–8.
10. Luo J, Nian J, Gao S. Stable apremilast crystalline form II free of solvate and method of making the same. 2017. US9850205B2.
11. Censi R, Di Martino P. Polymorph Impact on the Bioavailability and Stability of poorly soluble drugs. Molecules. 2015;20(10):18759–76.
12. Verma S, Rudraraju VS. A systematic Approach to Design and prepare solid dispersions of Poorly Water-Soluble Drug. AAPS PharmSciTech. 2014;15(3):641.
13. Liu J, Cao F, Zhang C, Ping Q. Use of Polymer combinations in the preparation of solid dispersions of a thermally unstable drug by hot-melt extrusion. Acta Pharm Sin B. 2013;3(4):263–72.
14. Muvva A, Lakshman D, Dwibhashyam VSNM, Dengale S, Lewis SA. In vitro-in silico evaluation of apremilast solid dispersions prepared via Corotating Twin Screw Extruder. J Drug Deliv Sci Technol. 2020;59:101844.
15. Tian Y, Qian K, Jacobs E, Amstad E, Jones DS, Stella L, et al. The investigation of flory-huggins interaction parameters for amorphous solid dispersion across the entire temperature and composition range. Pharmaceutics. 2019;11(8):420.
16. Zhao Y, Inbar P, Chokshi HP, Malick AW, Choi DS. Prediction of the thermal phase diagram of amorphous solid dispersions by flory-huggins theory. J Pharm Sci. 2011;100(8):3196–207.
17. Higuchi Takeru, Connors AL. Phase solubility techniques. In: Advanced Analytical Chemistry of Instrumentation, Vol. 4, 1965, pp. 117–212.
18. Lu J, Cuellar K, Hammer NI, Jo S, Gryczke A, Kolter K, et al. Solid-state characterization of Felodipine-Soluplus amorphous solid dispersions. Drug Dev Ind Pharm. 2016;42(3):485–96.
19. Thiry J, Krier F, Evrard B. A review of pharmaceutical extrusion: critical process parameters and scaling-up. Int J Pharm. 2015;479(1):227–40.
20. Gregory S, Jones BC, Singleton AH, Johnson WA. Tocopheryl polyethylene glycol succinate powder and process for preparing same. 2006. WO2007019058A1.
21. Hassan H, Adam SK, Alias E, Affandi MMRMM, Shamsuddin AF, Basir R. Central composite design for formulation and optimization of solid lipid nanoparticles to enhance oral bioavailability of acyclovir. Molecules. 2021;26(18):5432.
22. Saha SK, Joshi A, Singh R, Dubey K, ENHANCED SOLUBILITY, AND DISSOLUTION BY SURFACE-MODIFIED SOLID DISPERSION OF ALECTINIB HYDROCHLORIDE. Int J App Pharm. 2023;15(4):257–65.
23. Yang L, Wu P, Xu J, Xie D, Wang Z, Wang Q, et al. Development of Apremilast Solid Dispersion using TPGS and PVPVA with enhanced solubility and bioavailability. AAPS PharmSciTech. 2021;22(4):142.
24. Saha SK, Joshi A, Singh R, Jana S, Dubey K. An investigation into solubility and dissolution improvement of alectinib hydrochloride as a third-generation amorphous solid dispersion. J Drug Deliv Sci Technol. 2023;81:104259.
25. Crowley KJ, Zografi G. Water vapor absorption into amorphous hydrophobic drug/poly(vinylpyrrolidone) dispersions. J Pharm Sci. 2002;91(10):2150–65.
26. Saber RA, Attia AK, Salem WM. Thermal analysis study of antihypertensive drugs telmisartan and cilazapril. Adv Pharm Bull. 2014;4(3):283–7.
27. Lapuk SE, Zubaidullina LS, Ziganshin MA, Mukhametzyanov TA, Schick C, Gerasimov AV. Kinetic stability of amorphous solid dispersions with high content of the drug: a fast scanning calorimetry investigation. Int J Pharm. 2019;562:113–23.
28. Pandi P, Bulusu R, Kommineni N, Khan W, Singh M. Amorphous solid dispersions: an update for preparation, characterization, mechanism on bioavailability, stability, regulatory considerations and marketed products. Int J Pharm. 2020;586:119560.
29. Vay K, Scheler S, Friess W. Application of Hansen solubility parameters for understanding and prediction of drug distribution in microspheres. Int J Pharm. 2011;416(1):202–9.
30. Theeuwes F, Hussain A, Higuchi T. Quantitative analytical method for determination of drugs dispersed in polymers using differential scanning calorimetry. J Pharm Sci. 1974;63(3):427–9.
31. Marsac PJ, Li T, Taylor LS. Estimation of drug-polymer miscibility and solubility in amorphous solid dispersions using experimentally determined interaction parameters. Pharm Res. 2009;26(1):139–51.

32. Marsac PJ, Shamblin SL, Taylor LS. Theoretical and practical approaches for prediction of drug-polymer miscibility and solubility. Pharm Res. 2006;23(10):2417–26.

33. Effect Summary Report. https://www.jmp.com/support/help/en/18.0/index.shtml#page/jmp/effect-summary-report.shtml.

34. Pralhad T, Rajendrakumar K. Study of freeze-dried quercetin-cyclodextrin binary systems by DSC, FT-IR, X-ray diffraction and SEM analysis. J Pharm Biomed Anal. 2004;34(2):333–9.

35. Goddeeris C, Willems T, Houthoofd K, Martens JA, Van den Mooter G. Dissolution enhancement of the anti-HIV drug UC 781 by formulation in a ternary solid dispersion with TPGS 1000 and Eudragit E100. Eur J Pharm Biopharm. 2008;70(3):861–8.

36. Song IS, Cha JS, Choi MK. Characterization, in Vivo and in Vitro evaluation of solid dispersion of Curcumin containing d-α-Tocopheryl polyethylene glycol 1000 Succinate and Mannitol. Molecules. 2016;21(10):1386.

37. Xiong K, Ma X, Cao N, Liu L, Sun L, Zou Q, et al. Identification, characterization and HPLC quantification of impurities in apremilast. Anal Methods. 2016;8(8):1889–97.

38. Homayouni A, Sadeghi F, Varshosaz J, Afrasiabi Garekani H, Nokhodchi A. Promising dissolution enhancement effect of soluplus on crystallized celecoxib obtained through antisolvent precipitation and high pressure homogenization techniques. Colloids Surf B Biointerfaces. 2014;122:591–600.

39. Tong M, Wu X, Zhang S, Hua D, Li S, Yu X, et al. Application of TPGS as an efflux inhibitor and a plasticizer in baicalein solid dispersion. Eur J Pharm Sci. 2022;168:106071.

40. Patel NG, Serajuddin ATM. Moisture sorption by polymeric excipients commonly used in amorphous solid dispersion and its effect on glass transition temperature: I. Polyvinylpyrrolidone and related copolymers. Int J Pharm. 2022;616:121532.

41. Herbrink M, Vromans H, Schellens J, Beijnen J, Nuijen B. Thermal stability study of crystalline and novel spray-dried amorphous nilotinib hydrochloride. J Pharm Biomed Anal. 2018;148:182–8.